JOURNAL OF VIROLOGY, June 1994, p. 3702–3712
0022-538X/94/$04.00+0

Vol. 68, No. 6

The Protease of Herpes Simplex Virus Type 1 Is Essential for Functional Capsid Formation and Viral Growth

MIN GAO,[1]* LINDA MATUSICK-KUMAR,[1] WARREN HURLBURT,[1] SANDRA FEUER DiTUSA,[1] WILLIAM W. NEWCOMB,[2] JAY C. BROWN,[2] PATRICK J. McCANN III,[1] INGRID DECKMAN,[1] AND RICHARD J. COLONNO[1]

Department of Virology, Bristol-Myers Squibb Pharmaceutical Research Institute, Princeton, New Jersey 08543-4000,[1] and Department of Microbiology and Cancer Center, University of Virginia Health Science Center, Charlottesville, Virginia 22908[2]

Received 19 January 1994/Accepted 11 March 1994

The herpes simplex virus type 1 protease and related proteins are involved in the assembly of viral capsids. The protease encoded by the UL26 gene can process itself and its substrate ICP35, encoded by the UL26.5 gene. To better understand the functions of the protease in infected cells, we have isolated a complementing cell line (BMS-MG22) and constructed and characterized a null UL26 mutant virus, *m*100. The mutant virus failed to grow on Vero cells and required a complementing cell line for its propagation, confirming that the UL26 gene product is essential for viral growth. Phenotypic analysis of *m*100 shows that (i) normal amounts of the c and d forms of ICP35 were produced, but they failed to be processed to the cleaved forms, e and f; (ii) viral DNA replication of the mutant proceeded at near wild-type levels, but DNA was not processed to unit length or encapsidated; (iii) capsid structures were observed in thin sections of *m*100-infected Vero cells by electron microscopy, but assembly of VP5 into hexons of the capsid structure was conformationally altered; and (iv) nuclear localizations of the protease and ICP35 are independent of each other, and the function(s) of Na, at least in part, is to direct the catalytic domain N_o to the nucleus.

Herpes simplex virus type 1 (HSV-1) is an enveloped double-stranded DNA virus. Viral DNA is synthesized as concatemers in the nucleus of infected cells and processed into unit-length molecules, presumably at the time of encapsidation (16, 21). Three major types of capsids can be isolated from HSV-1-infected cells (12). They are designated A, B, and C, in order of increasing sedimentation distance in sucrose gradients. Type C capsids contain the viral genome and are able to mature into infectious virions. Type A and B capsids lack DNA and are found in the infected cell nucleus. Type A capsids are very similar to type C capsids in protein composition, while type B capsids differ in that they contain an additional polypeptide, ICP35 (infected cell protein 35), occupying the inner capsid space (1, 3, 16, 38). ICP35, also called VP22a or p40, comprises a family of proteins designated ICP35a through ICP35f (12–14). All forms of ICP35 can be detected by Western blots (immunoblots) of infected cell lysates, but only ICP35 forms e and f (ICP35ef) are present in B capsids (1, 29, 38). The abundance of ICP35 in B capsids (15 to 20% of the B-capsid protein) (12, 29, 30) and its absence from capsids after DNA encapsidation are analogous to what is observed with the scaffold protein of double-stranded DNA bacteriophage (4).

The capsid of HSV-1 is an icosahedral protein shell and is composed of 150 hexons and 12 pentons. In addition to ICP35 (VP22a), six other major proteins have been identified in B capsids: VP5, VP19C, VP21 (Nb), VP23, VP24 (N_o), and VP26. The capsid contains 960 copies of the major capsid protein, VP5, which is the structural subunit of both the hexons and the pentons of the capsomers (1, 31, 39, 44). There are approximately 1,100 molecules of ICP35 per capsid but only approximately 100 molecules of N_o and Nb per capsid (29, 30).

A temperature-sensitive (*ts*) mutant, *ts*1201, in which processing of ICP35cd to ICP35ef is dramatically reduced at the nonpermissive temperature (NPT), has been described (35). Although capsid structures were observed in mutant-infected cell lysates, the mutant failed to encapsidate viral DNA. Marker rescue experiments indicated that the lesions of *ts*1201 are located very near the N terminus of UL26 (36). The UL26 region of the HSV-1 genome is transcribed into two mRNAs which coterminate at the 3′ end but have different 5′ ends (15, 22, 27). The larger mRNA, the transcript of the UL26 gene, encodes 635 amino acids, while the smaller transcript (the UL26.5 gene) encodes 329 amino acids of ICP35, initiating at a methionine residue which corresponds to residue 307 of the UL26 coding region (22). Thus, the two proteins have identical sequences at the C-terminal 329 amino acids of the open reading frame. Genetic and functional analyses clearly demonstrated that the UL26 gene encodes a protease (Pra) that cleaves ICP35, the product of the UL26.5 gene (23–25) (Fig. 1). In transient transfection and *Escherichia coli* expression systems, the plasmid encoding Pra, the full-length protease, could specifically cleave ICP35 between Ala and Ser, 25 amino acids from its C terminus (5, 23–25, 36). Autoproteolysis of Pra also occurred at a site identical to this, since the sequence is the same as that found in ICP35. Another conserved autoproteolysis site was identified in the homologous protease gene product of cytomegalovirus, and cleavage at this site releases the catalytic domain of the protease (47). Both autocleavage site sequences are conserved in all known herpesviruses, and for HSV-1, the autoproteolysis occurs between residues 247 (Ala) and 248 (Ser) to generate Na and N_o (VP24) and between residues 610 (Ala) and 611 (Ser) (8, 23–25) (Fig. 1A). These sites have been called release and maturation sites, respectively (45). Direct amino acid sequence analysis with gel-isolated capsid proteins and an *E. coli* expression system

* Corresponding author. Mailing address: Department of Virology, Bristol-Myers Squibb Pharmaceutical Research Institute, P.O. Box 4000, Princeton, NJ 08543-4000. Phone: (609) 252-6467. Fax: (609) 252-6058.

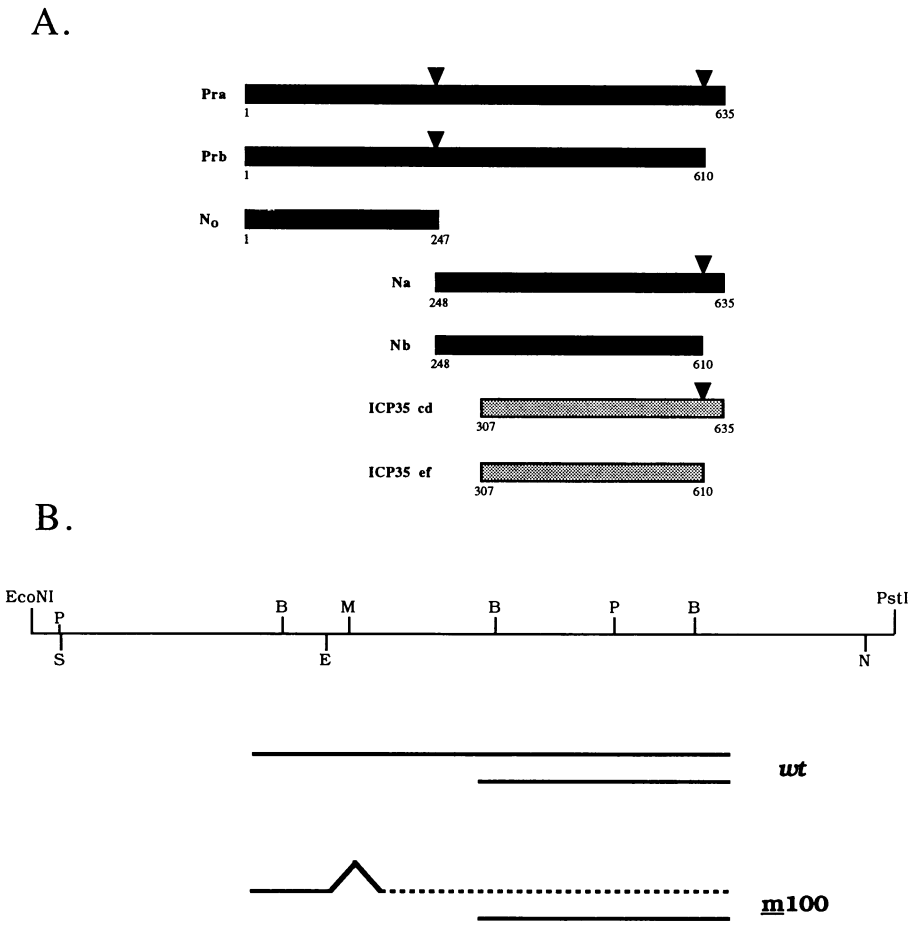

FIG. 1. (A) Polypeptide products of UL26 and UL26.5 open reading frames. The HSV-1 protease (Pra); substrate (ICP35cd); and cleavage products Prb, N_o (VP24), Na, Nb (VP21), and ICP35ef (VP22a) are described in the text. The sites of cleavage of Pra and ICP35cd are indicated by arrowheads. The UL26 amino acid residues at the N and C termini of each protein are indicated. (B) The UL26 and UL26.5 open reading frames of HSV-1 wt and mutant *m*100 genomes. The plasmid pRB4057 containing the UL26 and UL26.5 genes (*Eco*NI-*Pst*I fragment) was kindly provided by B. Roizman (23). Restriction enzyme sites are shown on the top line. B, *Bam*HI; S, *Sph*I; N, *Nhe*I; P, *Pst*I; E, *Eco*47; M, *Msc*I.

confirmed that Nb originates within Pra, beginning at residue 248 (8, 32). The cytomegalovirus protease, in addition to cleaving its substrate, a counterpart of ICP35, and autoprocessing at the N-terminal release site and C-terminal maturation site, can also cleave its proteolytic domain, causing inactivation of the enzyme (2, 46). This site is not conserved in the HSV-1 protease, and cleavage of the catalytic domain (N_o) has not been observed. The precise role of the proteolytic and autoproteolytic processing of the protease during capsid assembly and maturation of the virion is unknown.

Although the role(s) of capsid proteins in assembly is not well understood, the ability to isolate viral mutants has allowed detailed analysis of the functions of some of these proteins (7, 33, 36, 48). *ts* mutants of VP5 and VP19c (33, 48), as well as null mutants of VP5 and VP23 (7), result in the absence of capsid structures under nonpermissive conditions. The amounts of viral DNA replicated in cells infected with these mutant viruses are comparable to those in wild-type (wt)-infected cells, but viral DNA is not processed into unit-length size from concatemers.

We recently used an *E. coli* coexpression system to characterize plasmids containing UL26 and UL26.5 genes having truncations and cleavage site lesions (26, 45). To test the biological effects of these and other UL26 mutations in the context of HSV-1 infection, we propose to introduce these mutations back to the viral genome. In this paper, we report the isolation and characterization of HSV-1 protease-complementing cell lines and the construction of a protease mutant *m*100 virus.

MATERIALS AND METHODS

Cells and viruses. BHK21 clone 13 cells were grown and maintained as described by Preston et al. (36). Vero cells were grown and maintained as described previously (18). The growth medium for the neomycin-resistant cell lines BMS-MG22 and X4 (see below) included 250 μg of the antibiotic G418 per ml.

The HSV-1 wt strain KOS1.1 and the HSV-2 wt strain 186 were propagated and assayed as described previously (18, 20). The mutant viruses *ts*Prot.A and *m*100 were grown in the protease-expressing BMS-MG22 cell line.

Plasmids. The plasmid pRB4057 of HSV-1 strain F was kindly provided by B. Roizman (University of Chicago). The protease and ICP35 specified by pRB4057 carrying the wt *Eco*NI-*Kpn*I fragment are located between 0.325 and 0.55 map units (23). Plasmid pm100 was derived from pRB4057 by the deletion of a 91-bp *Eco*47III-*Msc*I fragment. pM307L was also

derived from pRB4057 by changing CCCATGAAC (Pro-Met-Asn) to CCTTTAAAC (Pro-Leu-Asn) by standard PCR techniques. Therefore, pM307L encodes the HSV-1 protease with the Met-to-Leu change at residue 307 (M307L). Since residue 307 (Met) of the protease is also the start codon for ICP35, the mutation should eliminate the synthesis or translation of ICP35. In addition to the desired base substitution for the M307L change, the silent mutation also generated a unique *Dra*I site. Mutations in pM307L were confirmed by DNA sequencing. Plasmid pRB4057ts was constructed as follows. First, a PCR fragment containing the Y30F mutation was generated by using the 5′ primer 5′-TGTGGGTGCGCCCAT GGCAGCCGAT-3′ and the 3′ primer 5′-CCGTATCCGG ATCCAATGCCAACTCGCCCGAGTCCCCGCTGTCAAA CAGG-3′; secondly, a PCR fragment containing the A48V mutation was generated by using the 5′ primer 5′-GGCATT GGATCCCGGATACGGTGCGGGCGGTCCTGCCTCCG G-3′ and the 3′ primer 5′-CCGAGGGCAGGTAGTTGG TGA-3′. After digestion of the first PCR product with *Nco*I-*Bam*HI and the second PCR product with *Bam*HI-*Sal*I, these two fragments were ligated into *Nco*I-*Sal*I sites of pGST247 (9). To generate pRB4057ts, three fragments (a 508-bp *Bsa*AI-*Sfi*I fragment containing *ts* mutations from pGST247, a 1,354-bp *Sfi*I-*Asp*718 fragment of pRB4057, and a 4,338-bp partial *Bsa*AI-*Asp*718 digestion fragment of pRB4057) were ligated. Mutations in pRB4057ts were confirmed by DNA sequencing. $pSVN_0$ was constructed by ligating the *Xba*I-*Kpn*I fragment (865 bp) of pT7247 (45) into pJ3Ω (28). pSVPra was constructed by ligating the *Sac*I-*Kpn*I fragment of pRB4057, containing the UL26 gene (22), into the *Sac*I-*Kpn*I sites of $pSVN_0$. Thus, expression of N_0 and Pra is under the control of the simian virus (SV40) early promoter.

Construction of *ts*Prot. We (5, 8, 9, 26, 45) and others (22–25) have performed studies with the HSV-1 protease and its substrate ICP35 expressed from strain F. To maintain consistency, we would like to construct a protease null mutant of strain F. However, strain F itself is a *ts* mutant (19) and cannot be used as our parental virus to construct the protease null mutant. Preston et al. recently disclosed that two amino acid substitutions in the protease of *ts*1201, Tyr to Phe at residue 30 and Ala to Val at residue 48, were encoded by the UL26 gene of *ts*1201 (HSV-1 strain 17) (35). Since the DNA sequences of the UL26 gene and its flanking regions are highly conserved among HSV-1 strains KOS, F, and 17 (10, 27), we decided to introduce the lesions present in plasmid pRB4057, derived from strain F, into the viral genome of the KOS1.1 strain and examine whether the mutant would produce the same *ts* phenotype. After cotransfection of infectious wt HSV-1 DNA and linearized plasmid, pRB4057ts, BHK cells were maintained at 34°C for 12 h in an attempt to increase recombination frequency and then shifted down to 31°C for an additional 24 h. Putative recombinant viruses were identified by their ability to grow only at the permissive temperature (PT), 31°C, and not at the NPT, 39.5°C. Although several *ts* mutants were identified, only two of them exhibited the *ts*1201 phenotype previously described (36, 37). These two isolates, named *ts*Prot.A and *ts*Prot.B, were isolated from independent transfections.

Isolation of the protease-expressing cell lines. Vero cells were transformed with the plasmids pRB4057 or pM307L and pSVneo as described previously (6, 23, 42). G418-resistant colonies were grown in cultures and screened for their ability to complement the growth of *ts*Prot.A at the NPT. The cell clone BMS-MG22, derived from a culture transfected with plasmid pM307L, yielded the highest level of complementation (Table 1). X4 cells, derived from a culture transfected with plasmid pRB4057, yielded lower levels of complementation of *ts*Prot.A at the NPT (results not shown).

TABLE 1. Complementation of *ts*Prot.A by BMS-MG22 cells

Virus	Titer (10^8 PFU/ml)[a]			
	BMS-MG22		Vero	
	31°C	39.5°C	31°C	39.5°C
KOS1.1	9.8	8.2	6.2	6.8
*ts*Prot.A	14	11	8.4	0.008

[a] Plaque numbers were counted at 2 days p.i. for the 39.5°C assay and at 6 days p.i. for the 31°C assay.

Isolation of mutant *m*100 virus. The fact that the mutant *ts*Prot.A exhibited a *ts* phenotype similar to that of *ts*1201 (35, 36) and could be complemented well in BMS-MG22 cells would suggest that the HSV-1 proteases and their ICP35 substrates from different strains of HSV-1 may be functionally equivalent. We therefore decided to introduce mutations in our plasmids derived from strain F into the background of strain KOS1.1. A null mutant virus was constructed by cotransfection of X4 cells with infectious KOS1.1 DNA and plasmid pm100. The progeny viruses from the marker transfer were tested for their ability to grow in X4, BMS-MG22, and Vero cells. One of the more than 200 viruses tested could grow in BMS-MG22 but was unable to grow in Vero cells. This virus was designated *m*100.

Analysis of viral DNA and proteins. Viral DNA for marker transfer was prepared as described previously (11). For Southern blot analysis (41), DNAs were prepared and analyzed essentially as described by Shao et al. (40) from Vero or BMS-MG22 cells infected with the wt virus or *m*100 at a multiplicity of infection (MOI) of 10 PFU per cell.

For Western blot analysis of infected cell lysates, cell monolayer cultures were infected with KOS1.1 or *m*100 virus at an MOI of 10 and harvested as indicated below. Sodium dodecyl sulfate-polyacrylamide gel electrophoresis (SDS-PAGE) was performed as described previously (11, 45). The proteins were transferred by electrophoresis to nitrocellulose filters. Detection of immune complexes on blots by a Western blot procedure involving a color reaction for alkaline phosphatase activity was conducted as specified by the manufacturer (Promega Biotec, Madison, Wis.). The anti-ICP35 monoclonal antibody (MAb) MCA406 (1:10,000 dilution; Serotec, Oxford, England) was used to detect ICP35 and protease-related products Pra, Prb, Na, and Nb.

Electron microscopy. Infected cells to be examined by electron microscope were centrifuged into a small (0.3-ml) pellet, fixed with 2.5% glutaraldehyde in 0.1 M phosphate buffer (pH 7.4) for 24 h at 4°C, and postfixed with 2% OsO_4 for 1 h at 24°C. Pellets were then washed with water, dehydrated in graded concentrations of acetone, embedded in Epon 812, and cut into sections (~70 nm thick) with a Richert Ultracut E ultramicrotome. Sections were stained with a saturated solution of uranyl acetate in methanol (20 min at 60°C) and then with 0.25% lead citrate (2 min at 24°C) and examined with a JEOL 100CX transmission electron microscope operated at 80 keV.

Indirect immunofluorescence. Indirect immunofluorescence was performed as described previously (11). Antibodies employed were the anti-ICP35 MAb MCA406 (1:50 dilution), the anti-N_0 polyclonal antiserum N-term rAb (1:150 dilution) (45), the anti-VP5 MAbs 8F5 (1:30 dilution) (43) and 3B (1:100 dilution) (43), and rhodamine-conjugated goat anti-mouse antibody (1:100 dilution).

RESULTS

Isolation of protease-complementing cell line. Genetic analysis of UL26 and UL26.5 mutants clearly defined the catalytic domain of the protease and cleavage sites in the protease and its substrate ICP35 (8, 23, 37). Our overall objective is to determine what role the protease and proteolytic processing play during capsid assembly by characterizing HSV-1 mutant viruses containing defined mutations in the UL26 gene. It was expected that many protease mutants would have a lethal phenotype. To propagate such mutants, we therefore felt that it was important to isolate protease-complementing cell lines.

To facilitate isolation of these complementing cell lines, we constructed the HSV-1 protease *ts* mutant, *ts*Prot. Two isolates, *ts*Prot.A and *ts*Prot.B, were found to be the same as that described by Preston et al. (36, 37). The mutant virus grew at 31°C but not at 39.5°C (Table 1). Processing of ICP35, examined by Western blot analysis, indicated that conversion of ICP35cd to ICP35ef in *ts* mutant-infected Vero cells at the NPT was dramatically reduced in comparison with that in wt-infected cells. This difference was not seen at the PT (data not shown). Further analyses were performed with *ts*Prot.A.

We then used *ts*Prot.A to screen cell lines for their ability to complement the growth of the *ts* virus at the NPT. The cell line BMS-MG22, derived from cultures transfected with a plasmid, pM307L, encoding only HSV-1 protease, yielded the highest level of complementation (Table 1). X4 cells, derived from a culture transfected with a plasmid, pRB4057, encoding both protease and ICP35, yielded a lower level of complementation and smaller plaques than did BMS-MG22 cells at the NPT (results not shown). KOS1.1 formed plaques on all cell lines. Both BMS-MG22 and X4 cells were derived from a single cell colony and were chosen for further use.

Complementation of *ts*Prot.A in *trans*. We examined the ability of the catalytic domain (N_o) of the protease expressed from a transfected plasmid to complement the growth of *ts*Prot.A at the NPT. Vero cells were transfected with control DNA, the wt protease plasmid, or mutant plasmids. After 16 h posttransfection, cells were infected with *ts*Prot.A and allowed to undergo a cycle of infection at the NPT. Virus yield was measured by plaque assay on BMS-MG22 cells to determine complementation (Table 2). As expected, the wt protease expressed from the UL26 gene under its own promoter (pRB4057) or the SV40 early gene promoter (SVPra) complemented the growth of *ts*Prot.A. The protease with a Met-to-Leu change at residue 307 (pM307L) also complemented growth of *ts*Prot.A. However, the 247-amino-acid proteolytic domain of the protease ($pSVN_o$) failed to provide complementation, suggesting that Na, the C-terminal 388-amino-acid domain of the protease, has some functions required for viral growth.

Isolation of the protease mutant *m*100 virus. Because the BMS-MG22 cell line efficiently complemented the growth of *ts*Prot.A at the NPT, we expected that it would serve as an efficient host for the isolation of HSV-1 protease mutant viruses.

The protease mutant plasmid, pm100, was constructed by deletion of a 91-bp *Eco*47III-*Msc*I fragment of the UL26 coding region (Fig. 1B), which did not alter the expression of ICP35. Thus, pm100 encodes only the first 100 amino acid residues of the protease. The mutation in pm100 was transferred into the wt HSV-1 KOS1.1 genome by marker transfer. Over 200 plaques resulting from cotransfection of X4 cells were tested for their ability to grow on BMS-MG22 or X4 cells and not on Vero cells. One virus grew on BMS-MG22 and X4 but not on Vero cells. The mutant was plaque purified three times and designated *m*100.

TABLE 2. Ability of mutant protease plasmids to complement HSV-1 *ts*Prot.A

Plasmid transfected[a]	Expt no.	Virus yield (PFU/ml)[b]	Complementation index[c]
pUC18	1	6.0×10^1	1
	2	8.0×10^1	1
pRB4057 (wt)	1	3.4×10^4	567
	2	3.4×10^5	4,250
SVPra (wt)	1	1.8×10^4	300
	2	2.0×10^5	2,500
pM307L	1	2.4×10^4	400
	2	1.6×10^5	2,000
SVN_o	1	1.6×10^2	2.7
	2	2.0×10^3	25

[a] Vero cells were transfected with the plasmids indicated. At 20 h posttransfection, the cells were infected with 3 PFU of *ts*Prot.A per cell and incubated for a further 22 h at 39.5°C before being harvested.
[b] Determined by plaque assay with BMS-MG22 cells at 39.5°C.
[c] Expressed as virus yield relative to that for cells transfected with pUC18 DNA.

The recombinant viral genome was examined by Southern blot analysis to confirm that the appropriate mutation in *m*100 was a result of marker transfer from the UL26 gene plasmid pm100. Total viral DNA isolated from *m*100-infected Vero cells was digested with *Bam*HI, separated by agarose gel electrophoresis, and transferred to a nylon filter. The filter was hybridized with a gel-isolated fragment containing the wt UL26 gene as a probe (Fig. 2). wt HSV-1 DNA contains four

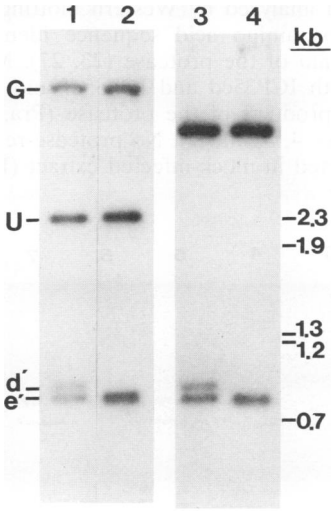

FIG. 2. Southern blot analysis of KOS1.1 and *m*100 genomes. Purified viral KOS1.1 (lane 1) and *m*100 (lane 2) DNAs were digested with *Bam*HI and subjected to electrophoresis in parallel with *Bam*HI-digested plasmid pRB4057 (lane 3) and pm100 (lane 4). Digested DNAs were separated on an 0.8% agarose gel, blotted onto a nylon membrane, and hybridized to a ^{32}P-labeled, gel-isolated *Nhe*I-*Sph*I fragment of pRB4057. The locations of molecular size markers are shown on the right. G, U, d′, and e′, *Bam*HI-G, -U, -d′, and -e′, fragments, respectively.

TABLE 3. Growth of mutant *m*100 virus

Virus	Titer (PFU/ml)[a]		Ratio (Vero/MG22)
	Vero	BMS-MG22	
wt	6.2×10^8	8.2×10^8	0.76
*m*100	$<2 \times 10^3$	2.2×10^8	$<9.1 \times 10^{-6}$

[a] Titers of viral stocks were determined by plaque assay with the cell lines indicated, and plaques were counted 2 days p.i.

hybridizing fragments, *Bam*HI-G, -U, -d′ (863-bp) and -e′ (797-bp) fragments (Fig. 2, lane 1). Identical *Bam*HI-d′ and -e′ fragments were also detected in *Bam*HI-digested plasmid pRB4057 (Fig. 2, lane 3). In contrast, the *m*100 DNA contained a new fragment of 772 bp because of the 91-bp deletion. This 772-bp new fragment overlapped with the 797-bp fragment (Fig. 2, lane 2). This deletion was also observed in *Bam*HI-digested plasmid pm100 (Fig. 2, lane 4), which was used for marker transfer to construct the mutant *m*100 virus. Thus, we conclude that the intended mutation has been introduced into the *m*100 genome.

Phenotype of *m*100. (i) Growth properties. Plaque assays were performed to determine whether the mutant *m*100 was able to grow in Vero cells. As expected, *m*100 was unable to form plaques on Vero cells at the lowest dilution (Table 3) but efficiently formed plaques on BMS-MG22 cells. The plaque size and the plating efficiency of *m*100 on X4 cells were reduced in comparison with those on BMS-MG22 cells (results not shown). Because the UL26 gene is the only known intact viral gene resident in the BMS-MG22 cell line, the lethal defect of *m*100 is most likely complemented in *trans* by the protease expressed from the cell line.

(ii) The protease and ICP35 expressed by *m*100. The viral mutant *m*100 was analyzed for expression of protease-related polypeptides. Vero, BMS-MG22, or X4 cells were either mock infected or infected with virus, and cell extracts were prepared at 9 h postinfection (p.i.). Cell extracts were separated by SDS-PAGE and analyzed by Western blotting (Fig. 3). Because ICP35 has amino acid sequence identical with the C-terminal domain of the protease (23, 27), MAb MCA406 reacted with both ICP35cd and ICP35ef and several of the autoproteolytic products of the protease (Pra, Prb, Na, and Nb) (Fig. 3, lanes 4, 5, and 7). No protease-related polypeptides were detected in mock-infected extract (Fig. 3, lane 1),

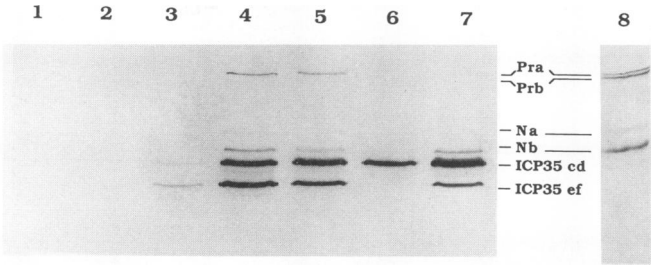

FIG. 3. Western blot analysis of HSV-1 protease-related polypeptides in wt- or *m*100-infected cells. Vero (lanes 4 and 6), BMS-MG22 (lanes 1, 2, 5, 7, and 8), and X4 (lane 3) cells were mock infected (lane 1) or infected with HSV-2 (lanes 2, 3, and 8), wt virus (lanes 4 and 5), or *m*100 (lanes 6 and 7). Total proteins were prepared at 9 h p.i., separated by SDS-PAGE, and transferred to a nitrocellulose filter. An approximately fivefold amount of HSV-2-infected BMS-MG22 cell extract was used for lane 8. The filter was probed with MAb MCA406, specific for ICP35.

indicating that BMS-MG22 cells did not express protease-related polypeptides constitutively. We were able to examine the expression of protease-related polypeptides expressed from BMS-MG22 and X4 cells after HSV-2 infection, since the MCA406 antibody recognizes HSV-1 ICP35 but not HSV-2 ICP35 (45). The amount of protease produced by BMS-MG22 cells was barely detectable (Fig. 3, lane 2). However, the production of the HSV-1 protease from BMS-MG22 cells was clearly detected when an approximately fivefold amount of HSV-2-infected cell extract was added for Western blotting (Fig. 3, lane 8), and no HSV-1 ICP35 was produced. In HSV-2-infected X4 cells, detectable amounts of ICP35cd were produced and processed into ICP35ef. However, the expression of ICP35 from X4 cells was obviously at a lower level than that from the wt virus (compare lanes 3 and 4 in Fig. 3). The reason for this is, at least in part, due to viral DNA synthesis: in the absence of viral DNA synthesis, the amounts of ICP35 were markedly reduced from the levels in wt-infected Vero cells (results not shown). Normal amounts of ICP35cd were produced in *m*100-infected Vero cells, but the proteins failed to be processed to ICP35ef (Fig. 3, lane 6), confirming that the deletion in *m*100 virus does not alter ICP35 expression. The protein migrating slightly faster than Nb in both wt- and *m*100-infected cells is most likely a different form of ICP35cd (3). ICP35cd was processed into ICP35ef by the protease provided in *trans* from *m*100-infected BMS-MG22 cells (Fig. 3, lane 7).

(iii) Analysis of viral DNA. We then examined the phenotype of *m*100 with regard to the replication and processing of viral DNA. Total viral DNA was isolated from mock-, wt-, or *m*100-infected Vero or BMS-MG22 cells at 15 h p.i. Equal amounts of DNA were digested with *Bam*HI, separated on an agarose gel, transferred to a nylon membrane, and hybridized with ^{32}P-labeled HSV-1 *Bam*HI-K junction fragment (Fig. 4A). Near-wt amounts of mutant *m*100 DNA (approximately 75% in this particular experiment) were detected in infected Vero cells (Fig. 4A, compare lanes 2 and 4). Slightly smaller amounts of mutant viral DNA synthesis were most likely due to experimental sample differences, since amounts of total DNA were judged by ethidium bromide staining. The ^{32}P-labeled *Bam*HI-K junction fragment hybridized not only to the junction fragment *Bam*HI-K but also to *Bam*HI-S and -Q end fragments, indicating that viral DNA was processed into the unit-length molecules in wt-infected Vero cells (Fig. 4A, lane 2). However, in *m*100-infected Vero cells, no *Bam*HI-S and -Q end fragments were observed, indicating that mutant viral DNA concatemers failed to be processed into unit-length molecules (Fig. 4A, lane 4). This defect was resolved in *m*100-infected complementing BMS-MG22 cells (Fig. 4A, lane 5). To confirm these results, DNase I-treated DNAs from wt- and *m*100-infected cells were analyzed (Fig. 4B). DNase I-resistant *Bam*HI-K, -S, and -Q fragments were detected in wt-infected Vero and BMS-MG22 cells, as well as in *m*100-infected BMS-MG22 cells (Fig. 4B, lanes 1, 2, and 4). No viral DNA was detected in *m*100-infected Vero cells (Fig. 4B, lane 3), suggesting that viral DNA concatemers of the *m*100 mutant were not encapsidated. From these experiments, we conclude that the mutant viral DNA replication proceeded at near the wt level but that DNA was not processed to the unit-length molecules and was not encapsidated.

(iv) Electron microscopic studies. Thin sections of virus-infected cells were examined by electron microscopy to determine whether mutant *m*100 formed capsids when grown in nonpermissive cells. Vero and BMS-MG22 cells were infected with the wt virus or *m*100, harvested, fixed with 2.5% glutaraldehyde at 16 h p.i., and prepared for electron microscopy as

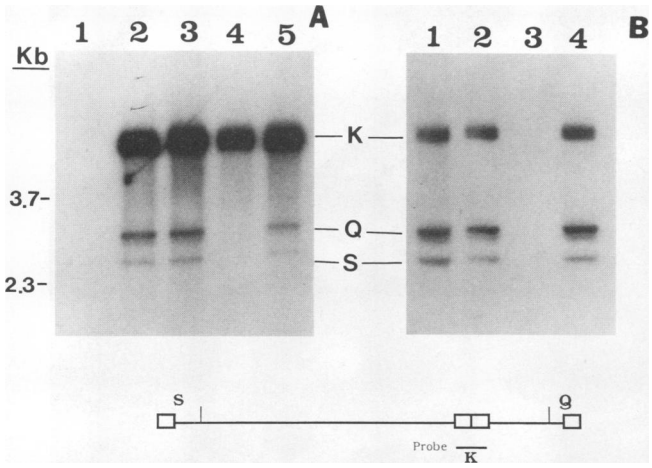

FIG. 4. Ability of the *m*100 mutant to process viral DNA. Vero cells or BMS-MG22 cells were mock infected or infected with wt HSV-1 or *m*100, and total DNA (A) or DNase I-treated DNA (B) was prepared at 16 h p.i. as described in Materials and Methods. Each DNA sample was digested with *Bam*HI, separated on a 0.8% agarose gel, blotted onto a nylon membrane, and hybridized to a ^{32}P-labeled *Bam*HI-K junction fragment. (A) Lanes: 1, mock-infected BMS-MG22 cells; 2, KOS-infected Vero cells; 3, KOS-infected BMS-MG22 cells; 4, *m*100-infected Vero cells; 5, *m*100-infected BMS-MG22 cells. (B) Lanes: 1, KOS-infected Vero cells; 2, KOS-infected BMS-MG22 cells; 3, *m*100-infected Vero cells, 4, *m*100-infected BMS-MG22 cells. The locations of molecular size markers are shown at the left. K, Q, and S, *Bam*HI-K, -Q, and -S fragments, respectively. The probe used in the hybridization experiments is diagrammed at the bottom.

described in Materials and Methods. Cells infected with wt HSV-1 were found to contain the three expected capsid types, A, B, and C, and virions (Fig. 5A). Although type A capsids were observed, they were not evident in the field shown in Fig. 5A. *m*100-infected cells were also found to contain large numbers of capsids, but all were of the electron-translucent (B-capsid) type (Fig. 5B). No dense-cored capsids were observed, indicating that viral DNA was not packaged in *m*100-infected cells.

(v) Recognition of VP5 in *m*100-infected Vero cells. It was recently reported that in the absence of the major capsid protein VP5, no capsid structures were observed by either electron microscopic or sucrose gradient sedimentation analysis (7). Since capsid structures were observed in *m*100-infected Vero cells, we would assume that VP5 would be part of the structures. Trus et al. showed that MAbs 8F5 and 3B appeared to recognize different conformationally dependent epitopes of VP5 in the B capsid (43). Results from cryoelectron microscopy and three-dimensional image reconstruction experiments indicated that MAbs 8F5 and 3B specifically bind to hexons and pentons of B capsids, respectively (43). To determine whether the failure to package viral DNA is due to the formation of nonfunctional B capsids, we tested the ability of these MAbs to recognize VP5 in *m*100-infected Vero cells.

Vero cells were infected with either *m*100 or the wt virus at an MOI of 20 PFU per cell and stained at 6 h p.i. with a VP5 MAb, 3B or 8F5. VP5 accumulated in the wt-infected cell nucleus, as judged by reactivity with either MAb 8F5 or MAb 3B (Fig. 6B and E). MAb 3B showed similar nuclear staining patterns of VP5 in wt-infected (Fig. 6E) and in mutant-infected (Fig. 6F) cells, indicating that assembly of VP5 into pentons was not affected in *m*100-infected Vero cells. The reduction of the intensity of the staining of VP5 with MAb 3B is not significant and was not observed in other repeated experiments. In contrast, MAb 8F5 recognized VP5 in wt-infected cells (Fig. 6B) but reactivity in mutant-infected cells was dramatically reduced (Fig. 6C), indicating that assembly of VP5 into hexons was affected and VP5 may have an altered conformation in mutant-infected cells. These findings suggested that the protease is required for formation of functional capsid structures.

Localization of HSV-1 protease-related proteins. Liu and Roizman (25) reported that when coexpressed with ICP35 in transfected cells, the N-terminal domain of the protease, N_o, had proteolytic activity and was able to process ICP35. It is possible that the inability of N_o to complement the growth of *ts*Prot.A at the NPT (Table 2) is due to the fact that N_o could not localize to the nucleus. It has been shown by immunoelectron microscopy that ICP35 in *ts*1201-infected cells localized to the nucleus (38). However, localization of the protease is unknown, because the antibody used recognized the C-terminal 329 residues of the protease, which are identical to ICP35. To determine whether the protease and ICP35 localize in the nucleus, we first examined the localization of ICP35 in *m*100-infected Vero cells. ICP35 localized to the nucleus in the absence of the protease in *m*100-infected cells (Fig. 7A). To determine whether the protease and ICP35 can accumulate in the nucleus independently of each other and other viral proteins, we also examined the cellular distributions of wt and mutant proteases and ICP35 expressed in transfected cells under the control of the SV40 early promoter. Our results showed that ICP35 accumulated exclusively in the nucleus (Fig. 7B) and the protease (Pra) localized predominantly in the nucleus (Fig. 7C), indicating that the two proteins could localize into the nucleus independently of each other. The proteolytic domain of the protease (N_o), in contrast to Pra, showed approximately equal intensities for both cytoplasmic and nuclear staining (Fig. 7D). We therefore conclude that the function of the Na domain of the protease, at least in part, is to direct the catalytic domain, N_o, of the protease to the nucleus.

DISCUSSION

In this report, we describe the reconstruction of HSV-1 *ts*Prot.A and show how it was used for the isolation of permissive BMS-MG22 and X4 cell lines. An HSV-1 protease mutant, *m*100, was isolated and propagated in these cell lines. Processing of the protease and its substrate ICP35 was examined by Western blot analysis with a specific MAb. In addition, indirect immunofluorescence was used to study the nature of the capsids formed.

Complementation of the growth of *ts*Prot.A and *m*100 on BMS-MG22 cells indicated that the protease with a Met-to-Leu amino acid change at residue 307 retained all of the functional activity of the wt protease. The growth of *m*100 virus on a complementing cell line and its failure to grow on Vero cells confirmed that the HSV-1 protease is essential for viral growth in tissue culture. The requirement of the protease to support viral growth could be due to its ability to process ICP35. It is possible that processing of ICP35 is required for alteration of capsid conformation and allows DNA packaging to follow. Autoprocessing at the N-terminal site may serve to release the catalytic domain and enable it to exert its function during capsid formation. Self-cleavage at the C-terminal maturation site of the protease could be simply due to the fact that the protease shares identical amino acid sequence with ICP35 and may not necessarily have any biological relevance. Alternatively, the reason for the protease being essential for viral

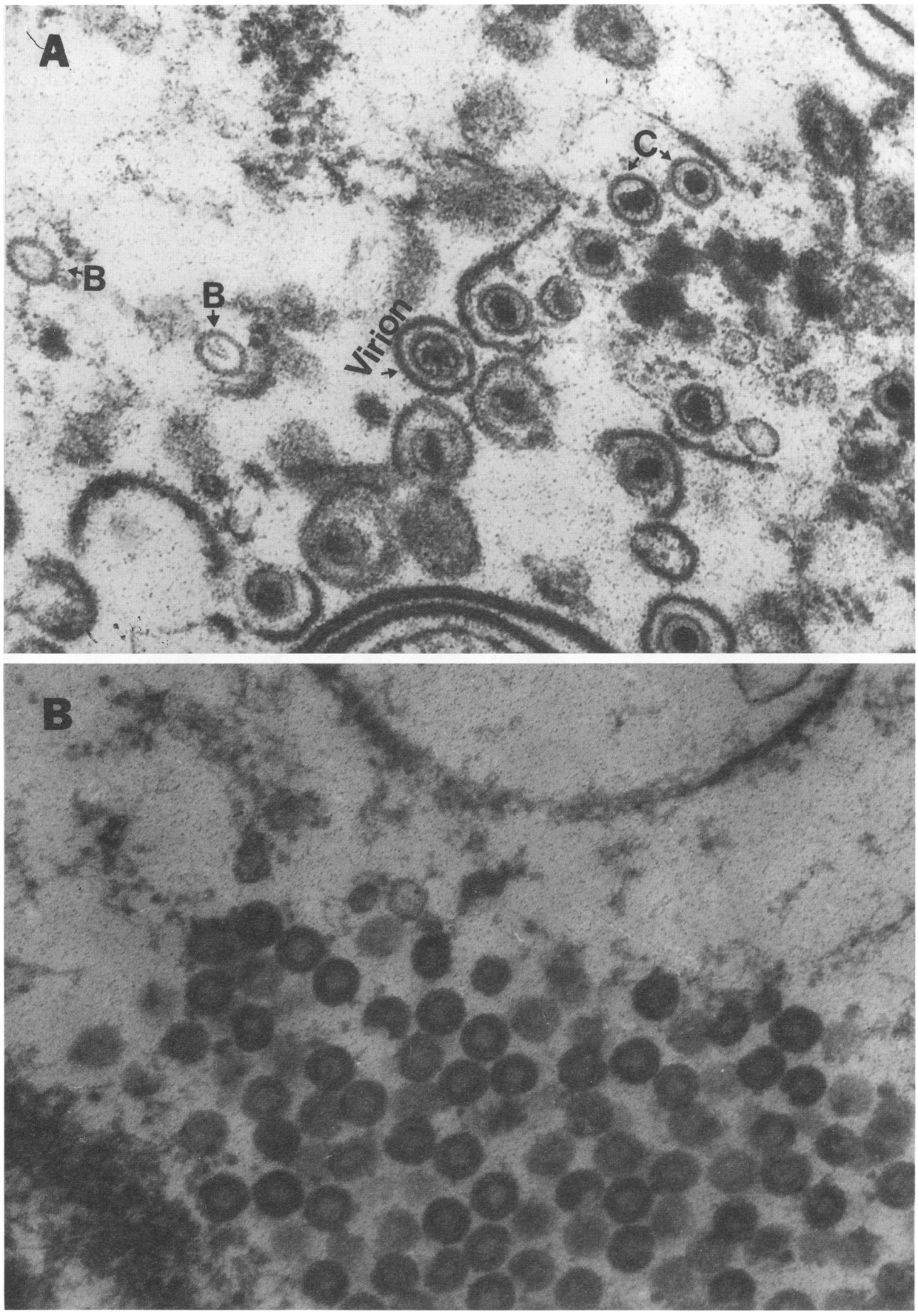
A
C
B
B
Virion
B

FIG. 5. Electron micrographs of thin sections of wt- and *m*100-infected cells. Vero cells were infected with the wt virus or *m*100 at an MOI of 10 PFU per cell. Cells were fixed and prepared at 16 h p.i. as described in Materials and Methods. (A) wt-infected Vero cells. Type B and C capsids and virions are labeled. (B) *m*100-infected Vero cells. Magnification, ×106,000.

growth could be that the catalytic domain (N_o) and Nb function structurally as part of capsids. In this case, both proteolytic processing and proteolytic products of the protease are essential for viral growth. Complementation of the growth of the *m*100 mutant by N- and/or C-terminal release site mutants will address some of these questions.

The absence of protease gene products in *m*100-infected cell lysates was confirmed by Western blot analysis with a MAb specific for ICP35. It was not surprising that *m*100, like other capsid protein mutants (7, 33, 36, 48), exhibited a wt phenotype for the amount of viral DNA replication under the nonpermissive condition. However, the replicated DNA in *m*100-infected Vero cells was not processed into unit-length molecules from concatemers. In addition to *m*100, other mutants with mutations in capsid genes specifying VP5, VP19c, and VP23 also failed to process concatemers to unit-length molecules (7, 33, 48). The fact that all of these proteins are involved in the assembly of capsid structures would suggest that the assembly of functional capsids is required for the processing of viral DNA. It has been reported recently that the UL15 gene product may be involved in viral DNA packaging (34) and that the alkaline nuclease is involved in the egress of capsids formed in the nucleus into the cytoplasm (40). In both cases, normal capsid structures were observed (34, 40).

Large aggregations of empty capsid structures were observed by electron microscopy in *m*100-infected Vero cells. Similar results were also observed in *ts*1201-infected cells at the NPT (36). In addition, like *ts*1201, ICP35cd was not processed into ICP35ef in *m*100-infected cells. However, unlike *ts*1201, *m*100 virus fails to generate any form of the protease. Western analysis of fractions from sucrose gradient sedimentation of *m*100-infected cell lysates indicated that unprocessed ICP35cd was present in the capsid structures, but only a small portion of the capsids containing ICP35 migrated into the gradient positions where wt capsids sedimented (10). These results suggest that *m*100 capsid structures may not be as stable as wt capsids. However, it is not yet clear whether this apparent instability is due to unprocessed ICP35cd in the capsid structure or to the lack of N_o and Nb.

Failure of the proteolytic domain N_o itself to localize into the nucleus demonstrated that at least one function of Na is to cause N_o to be found in the nucleus. The SV40 T antigen contains one of the best-defined nuclear localization signals (NLS), a highly basic sequence of amino acids (Pro-Lys-Lys-Lys-Arg-Lys-Val) (17). A region of basic amino acids (Gly-Lys-Arg-Arg-Arg-Tyr) has been located in the middle of the ICP35 polypeptide. This putative NLS is also shared by the protease in residues 425 to 430. It would be interesting to determine whether the nuclear localization and biologic functions of Pra can be restored when the NLS of the SV40 T antigen or the putative NLS of ICP35 is inserted into N_o. However, we do not think this could be the only reason why N_o does not complement the growth of *ts*Prot.A. Partial nuclear localization of N_o (Fig. 7) and the ability to process ICP35 (25) suggested that the

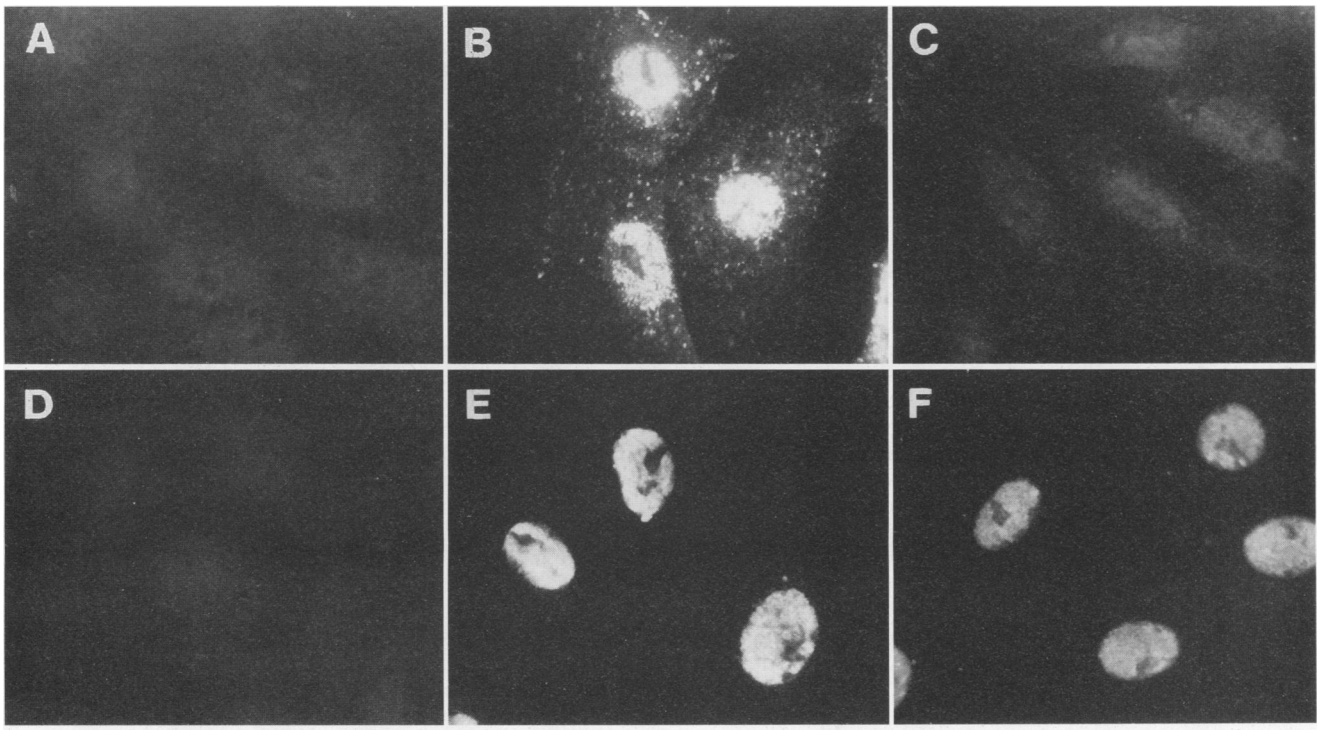

FIG. 6. Recognition of VP5 in *m*100-infected Vero cells. Vero cells were either mock infected (A and D) or infected with KOS1.1 (B and E) or *m*100 (C and F) and processed for indirect immunofluorescence at 6 h p.i. Cells were fixed, permeabilized, and incubated with anti-VP5 MAbs 8F5 (A, B, and C) and 3B (D, E, and F).

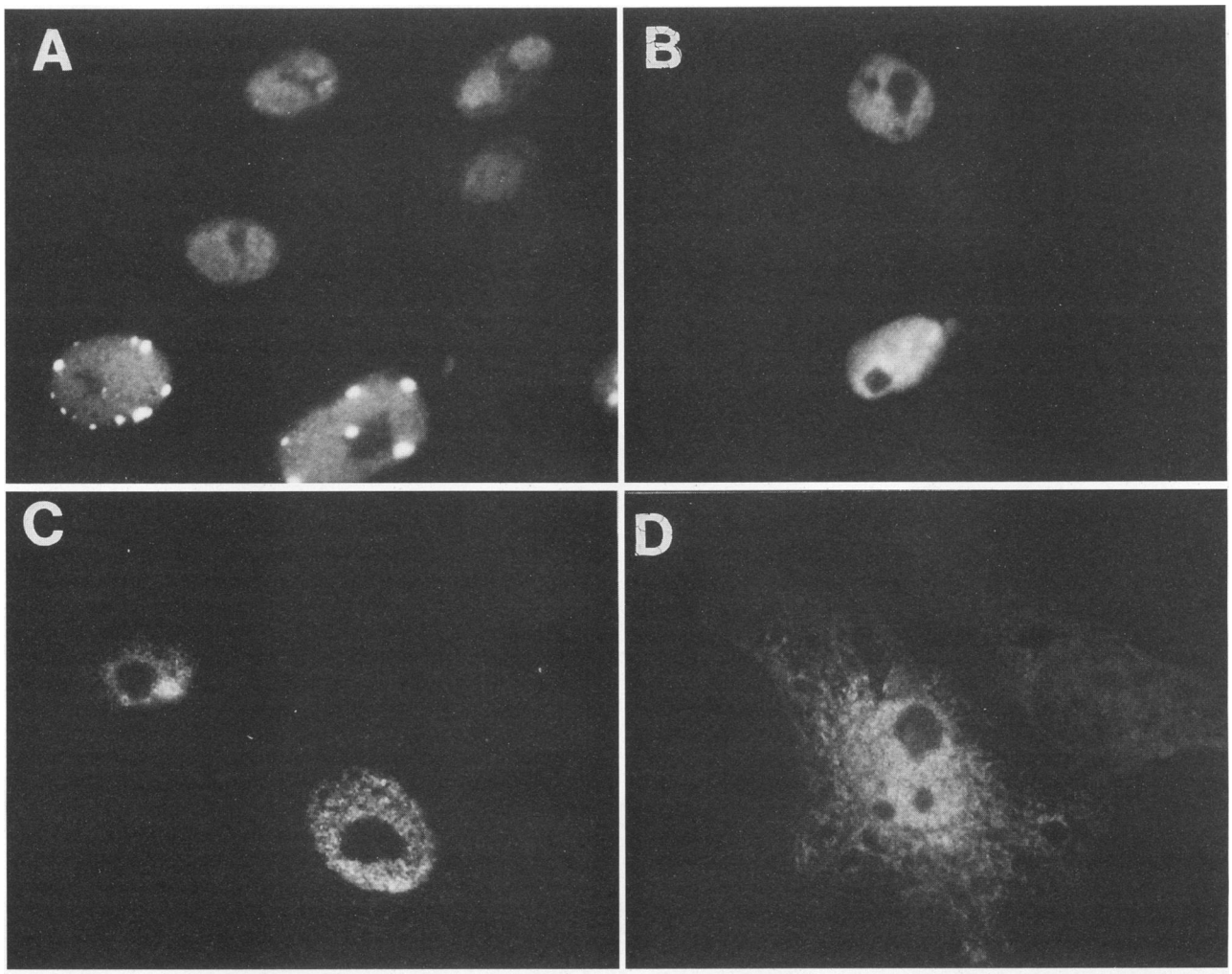

FIG. 7. Subcellular distribution of HSV-1 protease-related proteins. Vero cells were infected with *m*100 (A) and processed for indirect immunofluorescence at 6 h p.i. or transfected with pSVICP35 (B), pSVPra (C), or pSVN_o (D) and processed for indirect immunofluorescence at 18 h posttransfection. Cells were fixed, permeabilized, and incubated with anti-ICP35 MAb MCA406 (A and B) or anti-N_o polyclonal antiserum N-term rAb (C and D).

processing of ICP35 is not sufficient to support viral growth and that Na may have other functions in addition to directing N_o to the nucleus.

One possible function of Na is to interact with other proteins during the formation of capsids. Because the major portion of the Na amino acid sequence (residues 388 to 635) is identical to ICP35, Na may interact with the same proteins as ICP35. Alternatively, Na may have a conformation different from that of ICP35 prior to its release from the full-length protease and may therefore interact with proteins different from those with which ICP35 interacts.

The nuclear localization of the protease (Pra) observed in this study raised an interesting question regarding why N_o is not released into the cytoplasm by autoproteolysis of Pra. Our results strongly suggest that the N-terminal release site of Pra is protected from autoproteolysis when synthesized in the cytoplasm. Several possible explanations for this observation exist. One possibility is that Pra is rapidly transported into the nucleus prior to its autoproteolysis. Another possibility is that the cleavage sites, at least the N-terminal release site, are protected by the formation of a complex between the protease and other viral or cellular proteins. If this is the case, cellular proteins are most likely involved in the formation of the complex because, in transfected cells, Pra is the only viral protein present. Alternatively, the protection of Pra from autoproteolysis can be due simply to a different conformation of Pra when produced in the cytoplasm. For example, the N-terminal release site of Pra may not be exposed for cleavage in the cytoplasm. Finally, perhaps cleavage at the N terminus may not occur in *cis* and the Pra concentration in the cytoplasm may not be high enough for *trans* cleavage to occur.

Assembly of VP5 into the hexons of capsid structures may be altered in *m*100-infected cells, since reactivity of VP5 with MAb 8F5 was dramatically reduced. The protein epitope of MAb 8F5 is abundant in B capsids (960 copies) and was mapped to the distal tips of the hexon protrusions (43). It is conceivable that other parts of the hexons forming the basic matrix of the capsid shell may interact with the processed form of ICP35, ICP35ef, and, because of a conformational change, cannot be recognized on interaction with the unprocessed form, ICP35cd. Another MAb, 5C, which binds specifically to hexons but at a site that is quite different from that of the MAb

8F5 epitope (43), also reacted with VP5 only from wt-infected and not from *m*100-infected Vero cells (10). However, a third MAb (3B) reacts with VP5 from both wt- and *m*100-infected Vero cells. The epitope of MAb 3B is present at 60 copies per B capsid and was located at the outer rim of pentons (43). The epitope with which MAb 3B reacts may be located in a region of VP5 that does not undergo conformational change during maturation. The difference in antibody reactivities provides evidence that the protease ultimately affects assembly of capsid structures by influencing the conformation of VP5. Since VP5 accounts for about 60 to 70% of the mass of the surface shell (39, 44), a set of MAbs specific for VP5 (43) will provide useful means to study assembly of capsid structures.

ACKNOWLEDGMENTS

We thank Bernard Roizman for providing plasmid pRB4057 and Vallerie G. Preston for sharing data regarding *ts*1201 mutations prior to publication. We are grateful to Stanley Person, Prashant Desai, David M. Knipe, and Sandra K. Weller for helpful discussions. We thank Steve Weinhemer and other members of our group for their helpful discussions and comments on the manuscript.

This work was supported in part by a grant from the National Science Foundation (MCB-9119056) to J.C.B.

REFERENCES

1. **Baker, T. S., W. W. Newcomb, F. O. Booy, J. C. Brown, and A. C. Steven.** 1990. Three-dimensional structures of maturable and abortive capsids of equine herpesvirus 1 from cryoelectron microscopy. J. Virol. **64:**563–573.
2. **Baum, E. Z., G. A. Bebernitz, J. D. Hulmes, V. P. Muzithras, T. R. Jones, and Y. Gluzman.** 1992. Expression and analysis of the human cytomegalovirus UL80-encoded protease: identification of autoproteolytic sites. J. Virol. **67:**497–506.
3. **Braun, D. K., B. Roizman, and L. Pereira.** 1984. Characterization of posttranslational products of herpes simplex virus gene 35 proteins binding to the surfaces of full capsids but not empty capsids. J. Virol. **49:**142–153.
4. **Casjens, S., and J. King.** 1975. Virus assembly. Annu. Rev. Biochem. **44:**555–611.
5. **Deckman, I. C., M. Hagen, and P. J. McCann III.** 1992. Herpes simplex type 1 protease expressed in *Escherichia coli* exhibits autoprocessing and specific cleavage of the ICP35 assembly protein. J. Virol. **66:**7362–7367.
6. **DeLuca, N. A., A. McCarthy, and P. A. Schaffer.** 1985. Isolation and characterization of deletion mutants of herpes simplex virus type 1 in the gene encoding the immediate-early regulatory protein ICP4. J. Virol. **56:**558–570.
7. **Desai, P., N. A. DeLuca, J. C. Glorioso, and S. Person.** 1993. Mutations in herpes simplex virus type 1 genes encoding VP5 and VP23 abrogate capsid formation and cleavage of replicated DNA. J. Virol. **67:**1357–1364.
8. **DiIanni, C. L., D. A. Drier, I. C. Deckman, P. J. McCann III, F. Liu, B. Roizman, R. J. Colonno, and M. G. Cordingley.** 1993. Identification of the herpes simplex virus-1 protease cleavage sites. J. Biol. Chem. **268:**2048–2051.
9. **DiIanni, C. L., C. Mapelli, D. A. Drier, J. Tsao, S. Natarajan, D. Riexinger, S. M. Festin, M. Bolgar, G. Yamanaka, S. Weinheimer, C. A. Meyers, R. J. Colonno, and M. G. Cordingley.** 1993. In vitro activity of the herpes simplex virus-1 protease with peptide substrates. J. Biol. Chem. **268:**25449–25454.
10. **Gao, M., et al.** Unpublished data.
11. **Gao, M., and D. M. Knipe.** 1989. Genetic evidence for multiple nuclear functions of the herpes simplex virus ICP8 DNA-binding protein. J. Virol. **63:**5258–5267.
12. **Gibson, W., and B. Roizman.** 1972. Proteins specified by herpes simplex virus. VIII. Characterization and composition of multiple capsid forms of subtypes 1 and 2. J. Virol. **10:**1044–1052.
13. **Gibson, W., and B. Roizman.** 1974. Proteins specified by herpes simplex virus. Staining and radiolabeling properties of B capsids and virion proteins in polyacrylamide gels. J. Virol. **13:**155–165.
14. **Heilman, C. J., M. Zweig, J. R. Stephenson, and B. Hampar.** 1979. Isolation of nucleocapsid proteins of herpes simplex virus types 1 and 2 possessing immunologically type-specific and cross-reactive determinants. J. Virol. **29:**34–42.
15. **Holland, L. E., R. M. Sandri-Goldin, A. L. Goldin, J. C. Glorioso, and M. Levin.** 1984. Transcriptional and genetic analyses of the herpes simplex virus type 1 genome: coordinates 0.29 to 0.45. J. Virol. **49:**947–959.
16. **Jacob, R. J., L. S. Morse, and B. Roizman.** 1979. Anatomy of herpes simplex virus DNA. XII. Accumulation of head-to-tail concatemers in nuclei of infected cells and their role in the generation of the four isomeric arrangements of viral DNA. J. Virol. **29:**448–457.
17. **Kalderon, D., B. L. Roberts, W. D. Richardson, and A. E. Smith.** 1984. A short amino acid sequence able to specify nuclear location. Cell **39:**499–509.
18. **Knipe, D. M., M. P. Quinlan, and A. E. Spang.** 1982. Characterization of two conformational forms of the major DNA-binding protein encoded by herpes simplex virus 1. J. Virol. **44:**736–741.
19. **Knipe, D. M., W. T. Ruyechan, B. Roizman, and I. W. Halliburton.** 1978. Molecular genetics of herpes simplex virus: demonstration of regions of obligatory and nonobligatory identity within diploid regions of the genome by sequence replacement and insertion. Proc. Natl. Acad. Sci. USA **75:**3896–3900.
20. **Knipe, D. M., and A. E. Spang.** 1982. Definition of a series of stages in the association of two herpesvirus proteins with the cell nucleus. J. Virol. **43:**314–324.
21. **Ladin, B. F., M. I. Blankenship, and T. Ben-Porat.** 1980. Replication of herpesvirus DNA. V. Maturation of concatemeric DNA of pseudorabies virus to genome length is related to capsid formation. J. Virol. **33:**1151–1164.
22. **Liu, F., and B. Roizman.** 1991. The promoter, transcriptional unit, and coding sequences of the herpes simplex virus 1 family 35 proteins are contained within and in frame with the UL26 open reading frame. J. Virol. **65:**206–212.
23. **Liu, F., and B. Roizman.** 1991. The herpes simplex virus 1 gene encoding a protease also contains within its coding domain the gene encoding the more abundant substrate. J. Virol. **65:**5149–5156.
24. **Liu, F., and B. Roizman.** 1992. Differentiation of multiple domains in the herpes simplex virus 1 protease encoded by the UL26 gene. Proc. Natl. Acad. Sci. USA **89:**2076–2080.
25. **Liu, F., and B. Roizman.** 1993. Characterization of the protease and other products of amino-terminus-proximal cleavage of the herpes simplex virus 1 UL26 protein. J. Virol. **67:**1300–1309.
26. **McCann, P. J., D. R. O'Boyle II, and I. C. Deckman.** 1994. Investigation of the specificity of the herpes simplex virus type 1 protease by point mutagenesis of the autoproteolysis sites. J. Virol. **68:**526–529.
27. **McGeoch, D. J., M. A. Dalrymple, A. J. Davison, A. Dolan, M. C. Frame, D. McNab, L. J. Perry, J. E. Scott, and P. Taylor.** 1988. The complete DNA sequence of the long unique region in the genome of herpes simplex virus type 1. J. Gen. Virol. **69:**1531–1574.
28. **Morgenatern, J. P., and H. Lane.** 1990. A series of mammalian expression vectors and characterization of their expression of a reporer gene in stably and transient transformed cells. Nucleic Acids Res. **18:**1068.
29. **Newcomb, W. W., and J. C. Brown.** 1989. Use of Ar^+ plasma etching to localize structural proteins in the capsid of herpes simplex virus type 1. J. Virol. **63:**4697–4702.
30. **Newcomb, W. W., and J. C. Brown.** 1991. Structure of the herpes simplex virus capsid: effects of extraction with guanidine hydrochloride and partial reconstitution of extracted capsids. J. Virol. **65:**613–620.
31. **Newcomb, W. W., B. L. Trus, F. P. Booy, A. C. Steven, J. S. Wall, and J. C. Brown.** 1993. Structure of the herpes simplex virus capsid: molecular composition of the pentons and the triplexes. J. Mol. Biol. **232:**499–511.
32. **Person, S., S. Laquerre, D. Prashant, and J. Hempel.** 1993. Herpes simplex virus type 1 capsid protein, VP21, originates within the UL26 open reading frames. J. Gen. Virol. **74:**2269–2273.
33. **Pertuiset, B., M. Boccara, J. Cebrian, N. Berthelot, S. Chousterman, F. Puvion-Dutilleul, J. Sisman, and P. Sheldrick.** 1989. Physical mapping and nucleotide sequence of a herpes simplex

virus type 1 gene required for capsid assembly. J. Virol. **63:**2169–2179.

34. **Poon, A. P., and B. Roizman.** 1993. Characterization of a temperature-sensitive mutant of the U_L15 open reading frame of herpes simplex virus 1. J. Virol. **67:**4497–4503.
35. **Preston, V. G.** Personal communication.
36. **Preston, V. G., J. A. V. Coates, and F. J. Rixon.** 1983. Identification and characterization of a herpes simplex virus gene product required for encapsidation of virus DNA. J. Virol. **45:**1056–1064.
37. **Preston, V. G., F. J. Rixon, I. M. McDougall, M. McGregor, and M. F. Al Kobaisi.** 1992. Processing of the herpes simplex viral assembly protein ICP35 near its C-terminal end requires the product of the whole of the UL26 reading frame. Virology **186:**87–98.
38. **Rixon, F. J., A. M. Cross, C. Addison, and V. G. Preston.** 1988. The products of herpes simplex virus type 1 gene UL26 which are involved in DNA packaging are strongly associated with empty but not with full capsid capsids. J. Gen. Virol. **69:**2879–2891.
39. **Schrag, J. D., B. V. V. Prasad, F. J. Rixon, and W. Chiu.** 1989. Three-dimensional structure of the HSV-1 nucleocapsid. Cell **56:**651–660.
40. **Shao, L., L. M. Rapp, and S. K. Weller.** 1993. Herpes simplex virus 1 alkaline nuclease is required for efficient egress of capsids from the nucleus. Virology **196:**146–162.
41. **Southern, E. M.** 1975. Detection of specific sequences among DNA fragments separated by gel electrophoresis. J. Mol. Biol. **98:**503–517.
42. **Southern, P. J., and P. Berg.** 1982. Transformation of mammalian cells to antibiotic resistance with a bacterial gene under control of the SV40 early region promoter. J. Mol. Appl. Genet. **1:**327–341.
43. **Trus, B. L., W. W. Newcomb, F. P. Booy, J. C. Brown, and A. C. Steven.** 1992. Distinct monoclonal antibodies separately label the hexons or the pentons of herpes simplex virus capsid. Proc. Natl. Acad. Sci. USA **89:**11508–11512.
44. **Vernon, S. K., M. Ponce de Leon, G. H. Cohen, R. J. Eisenberg, and B. A. Rubin.** 1981. Morphological components of herpesvirus. III. Localization of herpes simplex virus type 1 nucleocapsid polypeptides by electron microscopy. J. Gen. Virol. **54:**39–46.
45. **Weinheimer, S. P., P. J. McCann III, D. R. O'Boyle II, J. T. Stevens, B. A. Boyd, D. A. Drier, G. A. Yamanaka, C. L. DiIanni, I. C. Deckman, and M. G. Cordingley.** 1993. Autoproteolysis of herpes simplex virus type 1 protease releases an active catalytic domain found in intermediate capsid particles. J. Virol. **67:**5813–5822.
46. **Welch, A. R., L. M. McNally, M. R. T. Hall, and W. Gibson.** 1993. Herpesvirus proteinase: site-directed mutagenesis used to study maturational, release, and inactivation cleavage sites of precursor and to identify a possible catalytic site serine and histidine. J. Virol. **67:**7360–7372.
47. **Welch, A. R., A. S. Wood, L. M. McNally, R. J. Cotter, and W. Gibson.** 1991. A herpes maturational proteinase, assemblin: identification of its gene, putative active site domain, and cleavage site. Proc. Natl. Acad. Sci. USA **88:**10792–10796.
48. **Weller, S. K., E. P. Carmichael, D. P. Aschman, D. J. Goldstein, and P. A. Schaffer.** 1987. Genetic and phenotypic characterization of mutants in four essential genes that map to the left half of HSV-1 UL DNA. Virology **161:**198–210.